A New Approach to Estimate Directional Spreading Parameters of a Cosine-2s Model

SHAOSONG ZHANG AND JUN ZHANG

Ocean Engineering Program, Civil Engineering Department, Texas A&M University, College Station, Texas

(Manuscript received 21 December 2004, in final form 13 July 2005)

ABSTRACT

For accurate and consistent estimates of the directional spreading parameter and mean wave direction of directional seas based on a cosine-2s directional spreading model, a new approach is proposed, employing a maximum likelihood method (MLM) to estimate the directional spreading function and then the angular Fourier coefficients. Because an MLM is more tolerant of errors in the estimated cross-spectrum than a directional Fourier transfer used in the conventional approach, the proposed approach is able to estimate the directional spreading parameter more accurately and consistently, which is examined and confirmed by applying the proposed approach and conventional approach, respectively, to the time series generated by numerical simulation and recorded in field measurements.

1. Introduction

Ocean waves are often directional and the information about wave direction and spreading around the mean wave direction is crucial to the applications of oceanography, and coastal and ocean engineering (Forristall and Ewans 1998). For example, wave direction and spreading play an important role in wave loads on offshore or coastal structures and the sediment transport in a surf zone. For simulating directional waves numerically or experimentally, a simple wave model, known as a cosine-2s model, has been widely used to describe waves spreading in a unimodal wave field where water waves at the same frequency spread around only one main direction although at different frequencies the main wave directions may be different (Hwang and Wang 2000). A directional wave spectrum can be described by $S(f, \theta) = S(f)D(\theta)$, where $S(f)$ is the energy density spectrum and $D(\theta)$ is the directional spreading function at frequency f. A cosine-2s model defines the spreading function by

$$D(\theta) = \kappa \cos^{2s}\left(\frac{\theta - \theta_M}{2}\right), \tag{1}$$

where κ is a normalization factor, θ_M the mean wave direction, and s the directional spreading parameter. Both θ_M and s depend on frequency f and are the key factors for the simulation of directional waves when a cosine-2s model is employed. Hence, the calibration and collection of various sea states in term of these two parameters are of great importance to wave climatology.

A general directional spreading function at frequency f can be expanded in an angular Fourier series,

$$D(\theta) = \frac{1}{\pi}\left(\frac{1}{2} + \sum_{n=1}^{\infty} A_n \cos n\theta + B_n \sin n\theta\right), \tag{2}$$

where A_n and B_n are the angular Fourier coefficients. In practice, directional waves are often measured by three or more wave sensors. Furthermore, three wave sensors at the same location are often deployed for measuring directional waves, for example, a pitch/roll buoy and the combination of a pressure transducer and a current meter. Based on three simultaneous wave measurements recorded at the same location, it is known that only the first and second angular Fourier coefficients can be obtained based on the cross-spectra using a method known as direct Fourier transfer (DFT) (Longuet-Higgins et al. 1963). In the case of the measurements recorded by a pitch/roll buoy,

$$A_1 = \frac{Q_{12}}{[C_{11}(C_{22} + C_{33})]^{1/2}}, \quad B_1 = \frac{Q_{13}}{[C_{11}(C_{22} + C_{33})]^{1/2}},$$
$$A_2 = \frac{C_{22} - C_{33}}{C_{22} + C_{33}}, \quad B_2 = \frac{2C_{23}}{C_{22} + C_{33}}, \tag{3}$$

where subscripts 1, 2, and 3 denote wave elevation; the x- and y-direction wave slope of the surface, respec-

Corresponding author address: Dr. Jun Zhang, Ocean Engineering Program, Dept. of Civil Engineering, Texas A&M University, College Station, TX 77843-3136.
E-mail: jun-zhang@tamu.edu

tively; and the real and imaginary parts C_{ij} and Q_{ij} of a cross-spectrum between wave records i and j. When the directional spreading function is described by a cosine-2s function, the spreading parameter s and the mean wave direction θ_M are related to the first harmonic through

$$s_1 = \frac{r_1}{1 - r_1}, \quad r_1 = \sqrt{A_1^2 + B_1^2}, \quad \theta_{M1} = \tan^{-1}\frac{B_1}{A_1}, \tag{4}$$

or to the second harmonic through

$$s_2 = \frac{1 + 3r_2 + \sqrt{1 + 14r_2 + r_2^2}}{2(1 - r_2)}, \quad r_2 = \sqrt{A_2^2 + B_2^2}, \quad \theta_{M2} = \frac{1}{2}\tan^{-1}\frac{B_2}{A_2}. \tag{5}$$

This approach has been widely used to determine the mean wave direction and spreading parameter. For example, wave data recorded by the National Data Buoy Center (NDBC) buoys are routinely processed using this approach (Earle 1996). In the following description, we name this approach as the conventional approach.

Ideally, if the directional spreading in ocean waves truly follows a cosine-2s model and the first two angular Fourier coefficients can be accurately computed based on the cross-spectra that are free from errors, then the spreading parameter and mean wave direction estimated, respectively, based on the first and second Fourier coefficient, should be identical, that is, $s_1 = s_2$ and $\theta_{M1} = \theta_{M2}$. Of course, the above "if" is not realistic and some differences between the two sets of estimates are expected. It is well documented that there are significant differences between s_1 and s_2, and s_2 is in general greater than s_1 (Hasselmann et al. 1980; Ewing and Laing 1987; Wang and Freise 1997). The data given by the database of NDBC (see information online at http://www.ndbc.noaa.gov/rmd.shtml) show that s_2 can be as great as twice s_1. Our tests conducted in this study show that even if a homogenous wave field is numerically generated following a cosine-2s model and is based on linear wave theory the estimated cross-spectra involve a random errors resulting from the "interaction" term (Jefferys 1987). Based on the statistics of this random error, Long (1980) approximately derived the standard deviations of s_1, s_2, θ_{M1} and θ_{M2} when the estimates are based on the measurements of a pitch–roll buoy using the conventional approach.

When the amplitude of the first and second Fourier coefficients (r_1 and r_2) approaches unity, the value of s_1 and s_2 become very large [see Eqs. (4) and (5)]. A small error in estimating the cross-spectra may be greatly amplified and results in an extremely large error in estimating the spreading parameter, as well as the significant inconsistency between estimated s_1 and s_2. In other words, the conventional approach is sensitive to errors in estimating the cross-spectra. To make the related estimates less sensitive to the errors in the cross-spectra, this study proposes an alternative method, namely, a data adaptive method, to estimate the angular Fourier coefficients and then the spreading parameter and mean wave direction. Applying it to numerically simulated wave records and field measurements, the proposed approach is found to be statistically superior to the conventional approach, especially in estimating the spreading parameter s.

In the next section, the statistics of the error resulting from the interaction term is quantified. The proposed approach to estimate s and θ_M is detailed in section 3. The superiority of the proposed approach over the conventional one is demonstrated in the cases of numerically simulated records in section 4 and in the cases of field measurements in section 5, respectively. Finally, the conclusions are given in section 6.

2. Errors in the estimation of cross-spectrum

The computation of the cross-spectra of a wave field is a prerequisite of estimating its directional spreading parameter and the mean wave direction. Errors related to estimated cross-spectra may result from noises occurring in measurements and assumptions made in computing wave characteristics, such as neglecting nonlinear wave interactions, wind, wave breaking, and the viscosity of water. In addition, the most common errors result from the so-called interaction term, which exists even in a homogenous wave field numerically generated based on linear wave theory. Because this type of error is significant and common to the estimated cross-spectra, and in turn to the predicted spreading parameter and mean wave direction, here we briefly show the source of the interaction term and the related measure for reducing its magnitude.

To simulate a linear and homogenous directional wave field, a single summation over the frequency domain is used to produce a resultant wave property by superposing the corresponding one of individual wave components:

TABLE 1. Linear transfer functions for different wave properties, where $\Gamma = \{\cosh[k(h + z)]/\cosh kh\}$ and $\Pi = 2\pi f\{\cosh[k(h + z)]/\sinh kh\}$.

Wave property	$H_m(\theta, f, z)$
Pressure	$\rho g\Gamma$
x-axis velocity	$\Pi \cos\theta$
y-axis velocity	$\Pi \sin\theta$
x-axis displacement	$i\Pi \cos\theta$
y-axis displacement	$i\Pi \sin\theta$

$$X_m(t) = \mathrm{Re}\sum_{j=1}^{\infty} H_m(f_j, \theta_j, \mathbf{x}, z)a_j e^{-i\psi_j}, \qquad (6)$$

where $\psi_j = \mathbf{k}_j \cdot \mathbf{x}_j - 2\pi f_j t_0 + \beta_j$, a_j and β_j are, respectively, the amplitude and initial phase of the jth component, and t_0 is the initial time; H_m stands for a linear transfer function from the elevation to the mth wave property. For example, the linear transfer functions used in this paper are listed in Table 1. Considering the fact that the numerically generated or measured wave records used in this study to determine the cross-spectra are of the same horizontal coordinates, without loss of generality, we may put the location of these records coincident with or below the origin of the Cartesian coordinates whose x and y axes are in the plane of the still water surface and z axis points upward. Hence, the horizontal coordinates of wave records disappear in the following equations.

To generate an ocean wave field consisting of numerous wave components whose frequencies vary almost continuously from low to high, the increment frequency Δf_g is chosen to be extremely small. That is, it is much smaller than the frequency increment used in the decomposition of a wave field into wave components $\Delta f_g \ll \Delta f_d = 1/T$, where T is the duration of the wave records used in the decomposition. The use of a single summation implies that simulated resultant waves are different in directions at different frequencies but are unidirectional at each discrete frequency, which seems to contradict the concept of wave directional spreading. The seemingly contradictory is resolved owing to $\Delta f_g \ll \Delta f_d = 1/T$, as elaborated below.

Based on the time series with limited duration T, the decomposed wave component at a discrete frequency defined by the fast Fourier transform (FFT) is the convolution of the actual wave components (of much finer resolution Δf_g in the frequency domain) and the Fourier transform of a window function of duration T,

$$F_m(f_k) = H_m a e^{-i\psi} \otimes W, \qquad (7)$$

where $\otimes$ denotes convolution. Various window functions, for example, rectangular and Hanning windows (Harris 1978), were employed in the digital signal processing. In the following equations, a rectangular window is used, which is also employed in our analysis of numerical simulation and field measurements. The Fourier transform of a rectangular window function is given by

$$W(f) = \frac{\sin\pi fT}{\pi fT} e^{-i\pi fT}. \qquad (8)$$

It is noted that the magnitude of W diminishes when $|f|$ increases. Hence, Eq. (7) can be approximated by

$$F_m(f_k) = \sum_{j=k-M}^{k+M} H_m(f_j, \theta_j, z)a_j e^{-i\psi_j} W(f_j - f_k), \qquad (9)$$

where M is a relatively large integer and $M\Delta f_g \le \Delta f_d < (M + 1)\Delta f_g$. The above equation indicates that the decomposed wave component of discrete frequency f_k is approximately equal to the superposition of $2M + 1$ wave components used in generating resultant wave field whose frequencies range from $f_k - M\Delta f_g$ to $f_k + M\Delta f_g$. These $(2M + 1)$ wave components are different in directions, and the directional spreading at frequency f_k can be approximately realized by appropriately choosing the directions of the $2M + 1$ wave components to follow a prescribed directional spreading function. Details about the implementation of the single summation model were described by Sand and Mynett (1987) and Miles (1989).

Using the Fourier coefficients of the wave properties m and n, the cross-spectrum between them at discrete frequency f_k is given by

$$\hat{\phi}_{mn} = \frac{1}{2}\sum_{j=k-M}^{k+M} H_m(f_j, \theta_j, z)H_n^*(f_j, \theta_j, z)w_j^2 a_j^2 + \delta\phi_{mn}, \qquad (10)$$

where

$$w_j = \frac{\sin\pi(f_j - f_k)T}{\pi(f_j - f_k)T},$$

$$\delta\phi_{mn} = \frac{1}{2}\sum_{j=k-M}^{k+M}\sum_{\substack{i=k-M\\ l\neq j}}^{k+M} H_m(f_j, \theta_j, z)H_n^*(f_l, \theta_l, z)w_j w_l a_j a_l e^{-i\Delta\psi_{jl}}, \qquad (11)$$

$$\Delta\psi_{jl} = \beta_j - \beta_l - \pi(f_j - f_l)(2t_0 + T), \qquad (12)$$

and * denotes the complex conjugate. The left-hand side of Eq. (10) is the estimated cross-spectrum and the first term at the right-hand side is approximately the true cross-spectrum. The second term $\delta\phi_{mn}$, known as the interaction term, is hence the discrepancy between

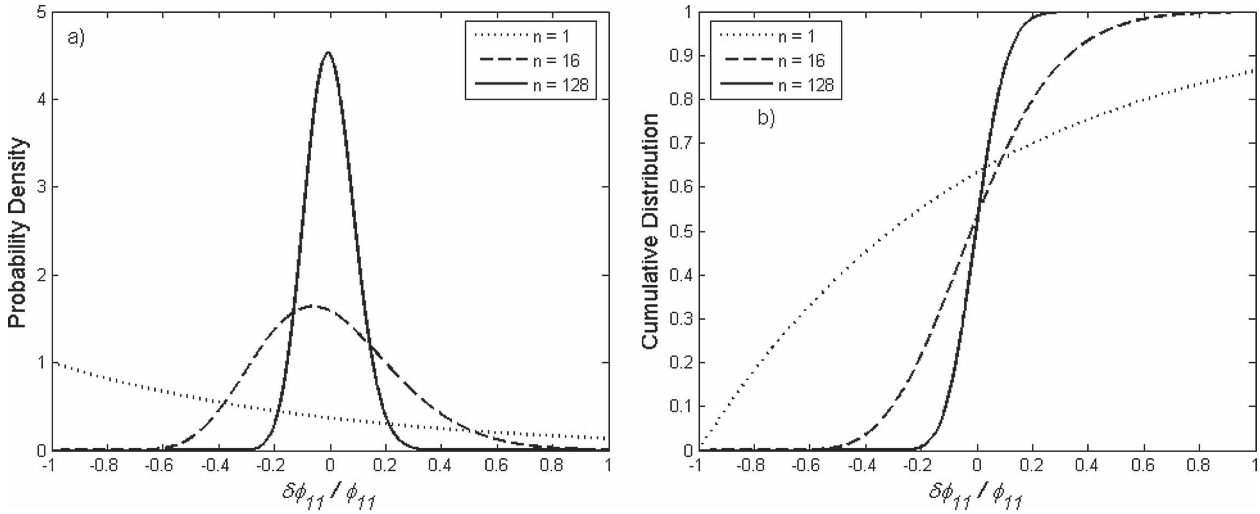

FIG. 1. (a) Probability density of $\delta\phi_{11}/\phi_{11}$, and (b) cumulative distribution of $\delta\phi_{11}/\phi_{11}$.

the true and estimated cross-spectrum. Because $\Delta\psi_{jl}$ is a random variable, the error $\delta\phi_{mn}$ behaves like a random variable as well. Its statistical properties were derived by Jenkins and Watts (1968). Although the mean of the error is equal to zero, for each individual realization (run) it is not likely to be zero, and indeed may not be very small. Their results were also confirmed in our numerical tests. For example, the normalized error $\delta\phi_{11}/\phi_{11}$ of the computed power spectrum from a single realization approximately obeys the *chi-squared* distribution $[(1/2)\chi_2^2 - 1]$ with 2 degrees of freedom, as plotted in Fig. 1a. In a single realization, the probability for $|\delta\phi_{11}/\phi_{11}| < 0.1$ is only about 0.0737, indicating that in more than 90% of the individual realizations the relative error is greater than 10%. To increase the probability for $|\delta\phi_{11}/\phi_{11}| < \varepsilon$, where ε is a small positive fraction, say 0.1, a common practice is to chop a time series of a wave record into a number of segments of the same duration T. A cross-spectrum is calculated based on a simultaneous set of segments belonging to a pair of wave records and then the corresponding cross-spectra of all segments are averaged to render the average cross-spectrum. The normalized error of the average power spectrum $\overline{\delta\phi_{11}}/\overline{\phi_{11}} \approx [(1/2n)\chi_{2n}^2 - 1]$ obeys the chi-squared distribution with $2n$ degrees of freedom, where n is the number of segments used in the average. The probability density functions for related chi-squared distributions of $n = 16$ and 128 are also plotted in Fig. 1a. It is shown that the variance of the normalized error is greatly reduced with the increase of n. For example, the probability that $|\overline{\delta\phi_{11}}/\overline{\phi_{11}}| < 0.1$ increases to 0.7429 when $n = 128$. In reality, however, the number of segments is limited because of the overall length of the measured wave records, and even if the measurements have durations much longer than 20 min the overall length of wave records used in the analysis has to be truncated in order to be consistent with the assumption of the stationary wave fields.

3. A new approach for estimating directional spreading

To obtain consistent and reliable estimation of unimodal directional seas in terms of θ_M and s, we propose a new approach based on the directional spreading function estimated using a data adaptive method. It was demonstrated that the directional spreading of a measured wave field could be estimated using data adaptive methods, such as the maximum likelihood method (MLM), maximum entropy method (MEM), and Bayesian method. Based on three simultaneous wave records, such as those measured by a pressure-current sensor (PUV) or a pitch–roll buoy, a conventional DFT method renders a directional energy spreading described by the first and second Fourier coefficients only while a data adaptive method is able to render a general approximate energy spreading. Because an MLM does not require prescribed (often subjective) parameters and its numerical scheme is relatively simple in comparison with an MEM or Bayesian method (Massel and Brinkman 1998), we use an MLM to estimate the directional spreading function. Three basic steps involved in our proposed approach are outlined in Fig. 2 and elaborated below.

At the beginning, the directional spreading function denoted by $D(\theta)$ is estimated using an MLM based on three or more simultaneous wave records following Isobe et al. (1984). In comparison with a prescribed

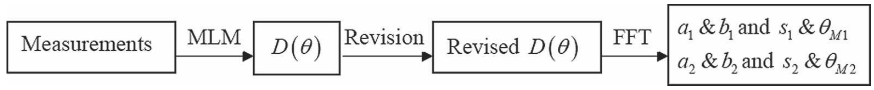

FIG. 2. Flowchart of the proposed approach.

unimodal wave spreading function following which a cross-spectrum matrix was generated and used as the input to the MLM, Isobe et al. (1984) found that the MLM slightly underpredicted wave energy around the mean wave direction while it overpredicted energy around the opposite direction. His observation was also confirmed in our related numerical tests.

Knowing the shortcomings of the MLM, in the second step we modify the estimated directional spreading function $D(\theta)$ to reduce the discrepancies. The modification is to cut wave energy nearby the opposite direction and then add to that around the mean direction. As sketched in Fig. 3, the cutoff angles, denoted by θ_L and θ_R, beyond which the wave energy is cut, are chosen based on two criteria: 1) the amount of wave energy cut beyond θ_L and θ_R is 7% of the total wave energy, and 2) wave energy at these two angles are equal, $D(\theta_L) = D(\theta_R)$. To conserve the total energy, the 7% energy cut in the tail is added back to the energy spreading function between θ_L and θ_R. The addition at a given direction θ is proportional to the value of $D(\theta)$ before the cut. Hence, the modification of energy spreading keeps the mean wave direction virtually unchanged and adds the wave energy mainly around the mean wave direction. It is noted that the modified energy spreading function abruptly reduces to zero at θ_L and θ_R. Because the discontinuities at these two directions do not play significant roles in determining the first and second

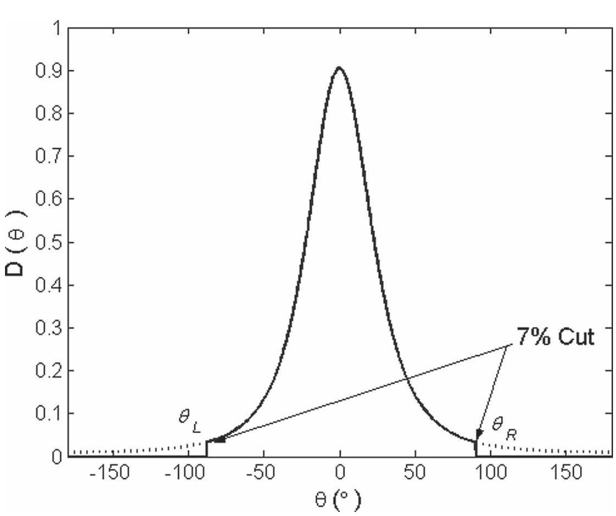

FIG. 3. Sketch of the modification of $D(\theta)$.

Fourier coefficients (for estimating θ_M and s) of modified directional spreading function, no effort was made to smooth them. It is also noted that the choice of the 7% cutoff energy in the tail is not a rigorous decision. Our numerical tests, however, show that the 7% cut works well in reducing the discrepancies between the directional spreading function predicted by the MLM and the corresponding cosine-2s function used as the input in for a wide range of s. It should be noted that the above modification to $D(\theta)$ might fail if the estimated directional spreading function is bi- or multimodal. Hence, the application of the proposed approach should be limited to sea states of unimodal directional spreading. At the third step, the first and second Fourier coefficients of the modified $D(\theta)$ are obtained using the FFT, and then the parameters s_1 and θ_{M1} or s_2 and θ_{M2} are calculated using Eqs. (4) and (5).

4. Application to numerically generated wave records

Before applying the proposed approach to the measurements of ocean waves, it is desirable to examine its accuracy and consistency under ideal conditions, that is, applying it to numerically simulated wave records that are free of measurement noises and errors because of the assumptions made in computing wave characteristics. Based on the time series of a wave field simulated following a cosine-2s spreading function of prescribed values of s and θ_M, the corresponding values of s and θ_M can be estimated using the proposed and conventional approach, respectively. The comparison between the estimated and the prescribed directional spreading parameter and mean wave direction may divulge the accuracy of the proposed approach and its superiority over the conventional approach. It is important to emphasize that the simulated wave records used as the input to the two approaches are time series recorded at a fixed point, resembling the measurements of ocean waves made by a pitch–roll buoy or a PUV. In some previous studies of data adaptive methods (e.g., Isobe et al. 1984; Hashimoto 1997), cross-spectra were calculated directly based on a prescribed directional spreading function and used as the input to numerical tests. Of course, the use of the cross-spectra directly calculated based on a prescribed directional spreading function avoids the error resulting from the interaction term as

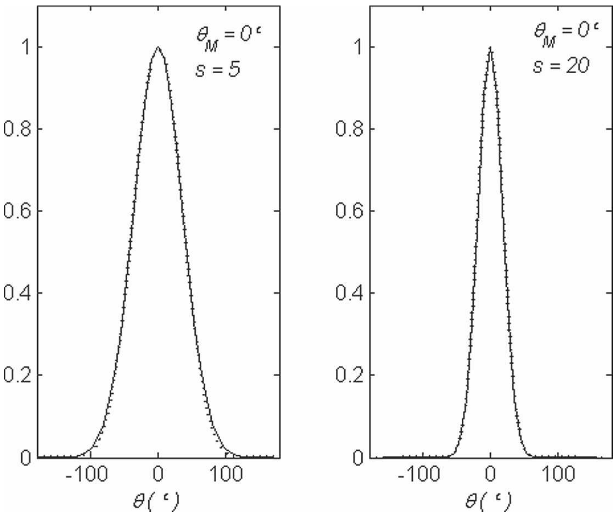

FIG. 4. Comparison of cosine-2s models with the corresponding normal distributions {large dots denote $\cos^{2s}[(\theta - \theta_M)/2]$; small dots denote $\exp[-((\theta - \theta_M)^2)/(4/s)]$}.

described in section 2, which may make the comparison look better. In our opinion, however, such numerical tests are unrealistic because the measurements of ocean waves in an overwhelming majority of cases are in the form of time series and its spreading function is not known in advance.

a. *Numerically generated time series*

To generate homogenous directional seas within the scope of linear theory, a single summation over the frequency domain is used to superpose individual wave components consisting of a directional wave field, as described in section 2. A directional irregular wave field of a prescribed cosine-2s spreading function at frequency $f_k = 11/128$ Hz is generated using 1025 wave components that are evenly distributed within the frequency band between 10/128 and 12/128 Hz ($\Delta f_g = 2^{-16}$ Hz and $M = 512$). Hence, the time series of the generated resultant wave field at a fixed point have nonrepeated durations of 65 536 s (about 18.2 h). The amplitude of these 1025 wave components are chosen to be the same and their initial phases are randomly selected between $-\pi$ and π. Making use of an approximation for large s (Tucker and Pitt 2001),

$$\cos^{2s}\frac{\theta - \theta_M}{2} \approx \exp\left[-\frac{(\theta - \theta_M)^2}{4/s}\right],$$

the directions of the 1025 components are randomly assigned following a normal distribution of the mean of θ_M and variance of $2/s$. Figure 4 shows that the above approximation holds well for $s > 5$.

In the following numerical tests, the time series of four resultant wave fields of different directional spreading parameters $s = 5$, 10, 15, and 20 are generated. These values of s cover the range of the spreading parameter of a majority ocean waves near their spectral peak frequencies (Mitsuyasu et al. 1975; Hasselmann et al. 1980). In all four resultant wave fields, the mean wave direction remains the same, $\theta_M = 0°$. It will be show that the use of the mean wave directions other than 0° does not substantially alter the findings made in our numerical tests. Once the time series of a directional wave field are generated, we apply the FFT to them and then obtain the related cross-spectra.

b. *Statistics of estimated spreading parameter and mean wave direction*

Each wave field of a prescribed spreading parameter was simulated 100 times, and each simulation (run) is realized by a set of randomly selected initial phases and directional angles as described in section 4a. In each run, the time series of wave-induced pressure and two horizontal velocity components were recorded at 5 m below the still water level and those of wave elevation and two wave slopes in the x and y axis were recorded at the still water level. It is understood that the wave slope at the still water level does not exist when the wave elevation is negative, and thus they are recorded as the extension of related wave slopes based on linear wave theory. Although the total nonrepeated duration of time series is about 18 h, we only use a 20-min section of time series in the numerical tests, resembling the length of most field measurements. Each time series is divided into 17 segments that are 128 s long with a 50% overlap. Because of the overlap, the equivalent degree of freedom (EDF) is reduced to 23 from 34 (Welch 1967). Applying the proposed and conventional approach, respectively, to the averaged cross-spectra, we obtain the estimated spreading parameter s and mean direction θ_M for each run of a resultant wave field. Based on the results of 100 runs of a simulated wave field, we are able to obtain the mean and variance of s_1, s_2, θ_{M1}, and θ_{M2} of each simulated wave field. The comparisons of the estimated and prescribed spreading parameter and mean wave direction based on the PUV records are similar to those based on the pitch/roll buoy records. For brevity, we only present the comparisons based on the pitch/roll buoy records in Tables 2–4. To confirm our computation on the statistics of the estimated spreading parameter and mean wave direction using the conventional approach, the corresponding ones calculated based on Long (1980), after a printing error in his equation for computing the standard deviation of s_1 was corrected, are also included in Tables 2

TABLE 2. Statistics of estimated θ_M ($s = 10$, $\theta_M = 0°$, EDF = 23).

Method	θ_{M1} (°)		θ_{M2} (°)	
	Mean	Std dev	Mean	Std dev
Long (1980)	0	5.402	0	6.994
Conventional approach	0.5260	6.437	0.5424	8.258
Proposed approach	0.5436	4.580	0.5700	5.051

TABLE 4. Std dev of the estimated s ($\theta_M = 0°$, EDF = 23).

	s_1			s_2		
s	Long	Conventional	Proposed	Long	Conventional	Proposed
5	1.97	2.00	1.34	2.89	2.86	1.33
10	4.25	4.38	2.79	5.19	5.25	2.81
15	6.84	7.02	3.12	7.93	8.06	3.13
20	9.21	8.89	5.03	10.53	10.20	5.05

and 4. His equations for computing the related statistics were derived based on the assumptions that the errors resulting from the interaction term obey a normal distribution and can be approximated by linearization. When the EDF is large enough, the chi-squared distribution becomes symmetric and closes to a normal distribution, as evidenced in Fig. 1a. Therefore, the standard deviations estimated using the conventional approach should be close to the corresponding ones computed based on Long (1980), which is confirmed in Tables 2 and 4.

It is found that the estimated mean directions of θ_{M1} and θ_{M2} by both approaches are consistent and in excellent agreement with the prescribed θ_M. For example, the statistics of the estimated mean wave direction given in Table 2 for the case of $s = 10$ and $\theta_M = 0°$ indicate that the accuracy of the mean wave direction predicted by both approaches is indeed excellent and the proposed approach produces slightly better results than the conventional approach. Consequently, our attention hereafter focuses on the comparisons of estimated and prescribed spreading parameters. As shown in Table 3, the mean of s_1 and s_2 predicted by both approaches is in satisfactory agreement with the corresponding prescribed value. It is noticed that the mean values of s_2 are consistently and noticeably greater than those of s_1 when they are estimated using the conventional approach. The proposed approach gives significantly smaller standard deviations of estimated s_1 and s_2 than the conventional approach, as shown in Table 4. The standard deviations of s_1 estimated using the proposed approach is about 42% in average smaller than those estimated using the conventional approach. In the case of s_2, the average reduction in the standard deviation is even greater, about 53%. It is also observed in Table 4 that the standard deviations of s_1 and s_2 estimated by both approaches increase with the increase in s, which is expected because when s is large it is very sensitive to a small change in Fourier coefficients. As a result, a small error in the average cross-spectrum may result in large error in the estimation of the spreading parameter.

TABLE 3. Mean of the estimated s ($\theta_M = 0°$, EDF = 23).

	s_1		s_2	
s	Conventional	Proposed	Conventional	Proposed
5	4.93	4.64	5.57	4.61
10	10.16	10.34	10.70	10.17
15	16.00	15.81	16.72	15.61
20	21.94	21.86	22.89	21.69

Large standard deviations of s_1 and s_2 may result in an inconsistency between estimated s_1 and s_2. This inconsistency was reported previously in using the conventional approach (Hasselmann et al. 1980; Ewing and Laing 1987). The large discrepancy between them was one of the major reasons to discard certain estimates of the spreading parameter of ocean waves (Wang and Freise 1997). To examine the consistency between them predicted by these two approaches, we plotted s_1 against s_2 of all runs of four simulated wave fields predicted by the conventional and proposed approach in Figs. 5a and 5b, respectively. Overall, the consistency between s_1 and s_2 shown in Fig. 5b is excellent because all points are close to the diagonal line, especially when the value of the prescribed spreading parameter is large. On the other hand, the consistency between s_1 and s_2 shown in Fig. 5a is unsatisfactory and in general s_2 is greater than s_1, especially in the cases of small prescribed spreading parameters. The inconsistency between s_1 and s_2 predicted using the conventional approach is not unique to the pitch/roll wave records. It was also observed in the case of PUV wave records.

Because the prescribed mean wave direction has been kept at zero in our numerical tests and one of recoded wave properties happens to be in the x direction, one may wonder whether the trend observed in the above comparison of the statistics will change if the prescribed mean wave direction is different from 0° or 90°. To answer this question, three additional prescribed mean wave directions (θ_M = 30°, 45°, and 60°) were used to simulate a resultant wave field of a prescribed spreading parameter $s = 15$. As in the previous numerical tests, 100 runs were performed for each prescribed mean wave direction. The related statistics are presented in Tables 5 and 6. They confirm that the statistics are virtually independent of the choice of prescribed mean wave direction.

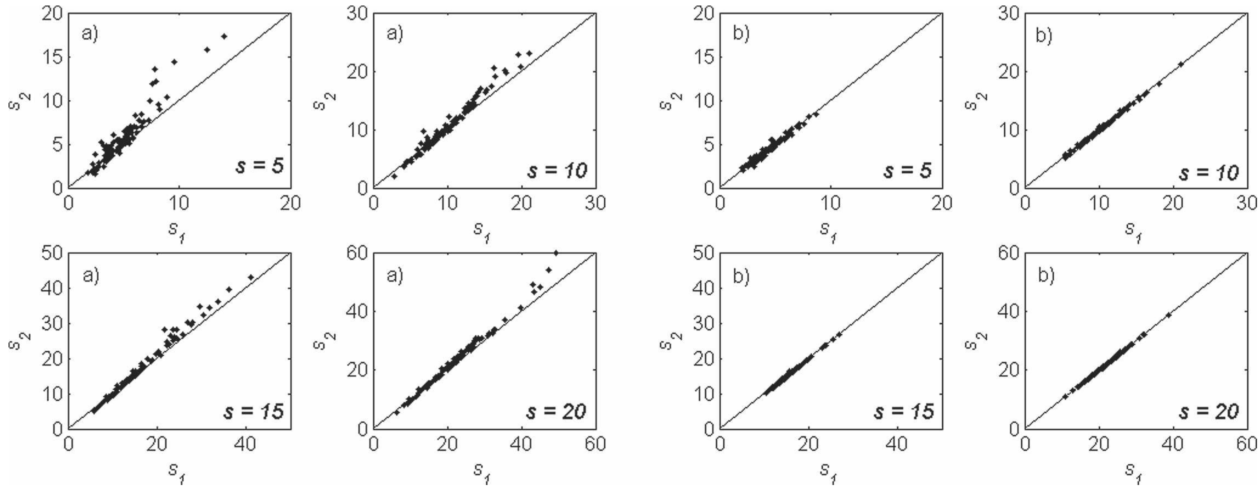

FIG. 5. The s_1 vs s_2 (EDF = 23) using the (a) conventional approach and (b) proposed approach.

To substantiate the results stated in section 2 that the probability for a small normalized error increases when the number of segments used in producing the average cross-spectra becomes greater, here we fully made use of the numerical time series of a duration of about 2 h. Each time series was divided into 111 segments of 128 s with a 50% overlap. Therefore, the corresponding average cross-spectra have the EDF of about 148. Given in Table 7 are the standard deviations of estimated s_1 and s_2 using the proposed and conventional approach, respectively. The standard deviations given by both approaches decrease significantly in comparison with those in Table 4. Furthermore, the standard deviations given by the conventional approach are closer to those of Long (1980), which is anticipated because of a much larger number of EDF (148) in this case. The consistency between s_1 and s_2 of all four resultant wave fields is plotted in Fig. 6a for the conventional approach and in Fig. 6b for the proposed approach. In comparison with Figs. 5a and 5b, Fig. 6a shows significant improvement in the consistency between s_1 and s_2 estimated using the conventional approach, while a smaller improvement is observed in Fig. 6b. The improvement observed in Table 4 and Figs. 6a and 6b shows that the reduction in the error of the estimated cross-spectra greatly reduces the errors in estimating the spreading parameter when the conventional approach is used but only marginally improves the estimates when the proposed approach is used. This observation suggests that the proposed approach is less sensitive to the errors involved in the estimated cross-spectra than the conventional approach. This advantage of the proposed approach becomes more crucial in its application to field measurements. It is because the computation of the cross-spectra based on field measurements involves errors resulting not only from factors other than the interaction term but also the duration of time series, namely, the number of cross-spectra used in producing their averages is limited because of the assumption of stationary seas.

5. Application to field measurements

The Wave Crest Sensor Intercomparison Study (WACSIS), a Joint Industrial Project, measured ocean waves in the southern North Sea during the 1997–98 stormy seasons. Various types of wave sensors were attached to a fixed platform located in water of 18-m depth and about 9 km off the Dutch coast. Among these sensors was a S4ADW current meter deployed 10 m below the mean sea level, measuring the two horizontal velocity components and pressure. Wave infor-

TABLE 5. Mean of estimated s and θ_M for different wave directions (s = 15, EDF = 23).

	s_1		s_2		$\theta_{M1} - \theta_M$ (°)		$\theta_{M2} - \theta_M$ (°)	
θ_M (°)	Conventional	Proposed	Conventional	Proposed	Conventional	Proposed	Conventional	Proposed
30	15.68	15.92	16.44	15.74	0.39	0.42	0.47	0.45
45	16.05	15.46	16.77	15.26	0.10	−0.07	0.32	−0.07
60	16.21	16.01	16.92	15.81	0.26	0.00	0.29	−0.02

TABLE 6. Std dev of estimated s and θ_M for different wave directions ($s = 15$, EDF = 23).

	s_1		s_2		θ_{M1} (°)		θ_{M2} (°)	
θ_M (°)	Conventional	Proposed	Conventional	Proposed	Conventional	Proposed	Conventional	Proposed
30	6.64	3.81	7.87	3.83	4.38	3.41	5.18	3.51
45	6.54	3.50	7.50	3.53	4.93	3.96	5.82	4.04
60	6.66	3.90	7.81	3.94	4.64	3.41	5.47	3.53

mation was also collected by a directional Waverider buoy measuring three components of wave-induced acceleration, which was moored about 1 km to the north of the platform. Comprehensive description of the WACSIS and its measurement are referred to in Forristall et al. (2004). The measurements recorded by the S4ADW and Waverider are used here to examine the accuracy and consistency of the two approaches in estimating the directional spreading parameter and mean wave direction. Because second-order wave–wave interactions mainly affect wave characteristics in the frequency ranges that are relatively low or high with respect to the spectral peak frequency (Zhang et al. 1996), to exclude the errors resulting from the neglect of second-order nonlinear wave–wave interactions in this study we mainly focus our attention to the estimate of the directional spreading parameter and mean direction of waves at the spectral peak frequency. It is known that the spreading parameter at the spectral peak reaches the maximum and decreases away from the peak frequency (Mitsuyasu et al. 1975; Hasselmann et al. 1980). To demonstrate the efficacy of the proposed approach not limited to the measurements at the spectral peaks, we also estimate the spreading parameters at frequencies at the entire frequency domain using both approaches. It should be noted that the estimate of the spreading parameters away from the spectral peak, especially at relatively high or low frequencies, can be further improved if the second-order bound waves are decoupled from the measurements, which will be conducted in our future study.

All available datasets recorded by the S4ADW and Waverider were screened based on the following three criteria. First, if a dataset involves a lot of abnormal spikes that were observed in some velocity records made by the S4ADW, the related dataset was excluded in this study. Second, when the velocity component of the ocean currents in the mean wave direction is significant with respect to the wave phase velocity at the spectral peak frequency, the observed (or appearance) wave frequency can be significantly different from the corresponding intrinsic frequency resulting from the Doppler effect, which may result in large errors in estimating wave directional spreading unless the effect of current is properly accounted for (Zhang and Zhang 2004). Hence, when the projected current velocity in the mean wave direction is greater than 5% of the phase velocity at the spectral peak, the related datasets were discarded. Third, the consistency between the estimated θ_{M1} and θ_{M2} is excellent if the directional spreading function of a wave field is of unimodal, as evidenced in our previous numerical tests. It is also known that the estimated mean wave directions (θ_{M1} and θ_{M2}) of a wave field of bi- or multimodal directional spreading are significantly different. Therefore, significant differences between them can be viewed as a vital sign of the sea states of bi- or multimode directional spreading. Hence, if the difference between the θ_{M1} and θ_{M2} estimated using the conventional approach is greater than 10°, the related wave field is thought to be bi- or multimodal and should not be modeled by a cosine-2s spreading function. The related datasets were consequently rejected as well. It is noted that the cases that were rejected because of the difference between θ_{M1} and θ_{M2} being greater than 10° are very few in the WACSIS datasets, accounting for about 3.4% of cases considered in our study.

After screening, we had 85 cases available to our

TABLE 7. Std dev of the estimated s ($\theta_M = 0°$, EDF = 148).

	s_1			s_2		
s	Long	Conventional	Proposed	Long	Conventional	Proposed
5	0.68	0.73	0.53	0.94	0.96	0.53
10	1.45	1.41	1.00	1.72	1.68	1.00
15	2.30	2.58	1.54	2.60	2.88	1.55
20	3.17	3.53	2.00	3.52	3.90	2.00

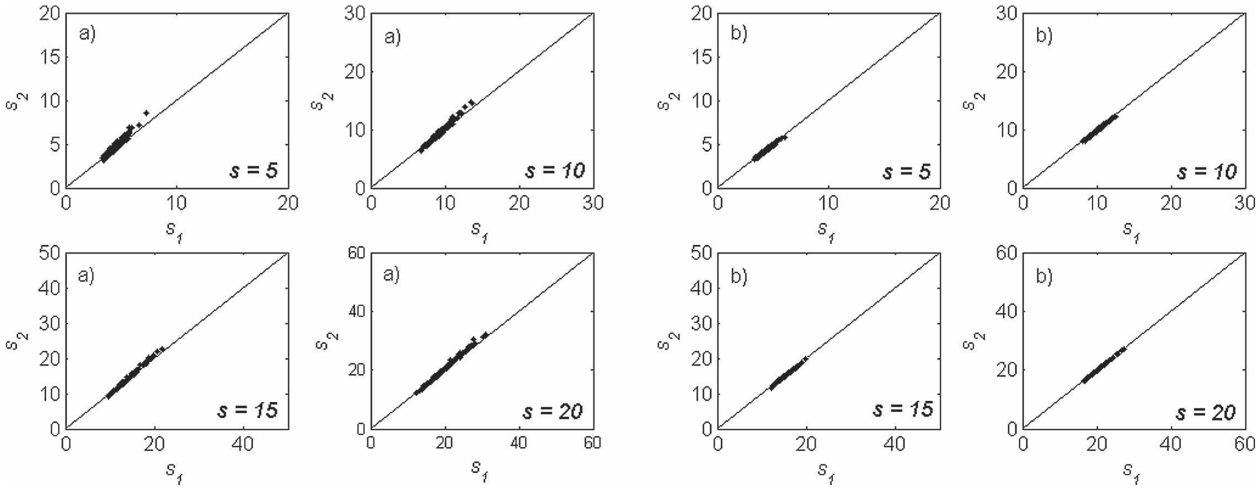

FIG. 6. The s_1 vs s_2 (EDF = 148) using the (a) conventional approach and (b) proposed approach.

study, each of which was recorded by both S4ADW and Waverider. The related datasets were used as the input to the two approaches for the estimate of the spreading parameter and mean wave direction. The ratio of the projecting current to the phase velocity and the significant wave height of 85 selected cases are summarized in Fig. 7. Each dataset involves a 20-min time series of a sampling rate at 2 Hz. Similar to our numerical tests, for obtaining the average cross-spectra each 20-min time series was divided into 17 segments of a 128-s duration with a 50% overlap between two consecutive segments.

a. Datasets recorded by the directional Waverider buoy

Unlike a pitch–roll buoy measuring the vertical acceleration and two wave slopes in the x and y directions, the directional Waverider buoy measures three acceleration components (vertical, north, and west). Three measured acceleration components were then integrated twice in the time domain to render three corresponding components of the particle displacement, which were given in the WACSIS database. Consistent with linear wave theory, we assumed that the three components of the displacement were recorded at a fixed point at the mean sea level. The first and second Fourier coefficients of the directional spreading function of a measured wave field were calculated following Eq. (3) in using the conventional approach.

The spreading parameters s_1 and s_2 and mean wave directions θ_{M1} and θ_{M2} at the spectral peaks, estimated using the two approaches, respectively, are compared in Figs. 8 and 9. Similar to the trend observed in the re-

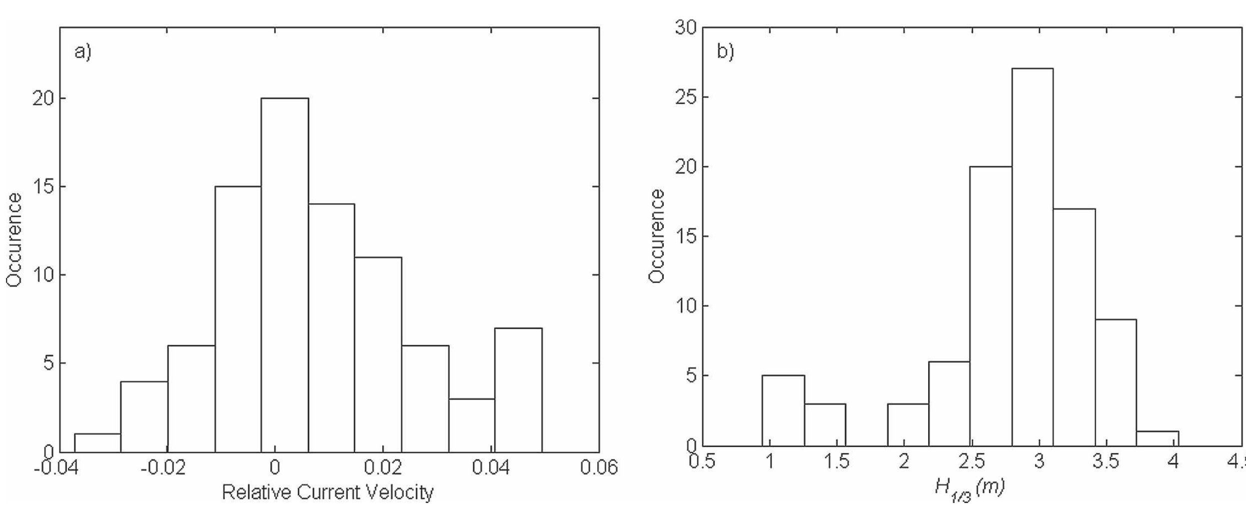

FIG. 7. Histogram of (a) the ratio of the projecting current velocity in the mean wave direction to the phase velocity, and (b) the significant wave height.

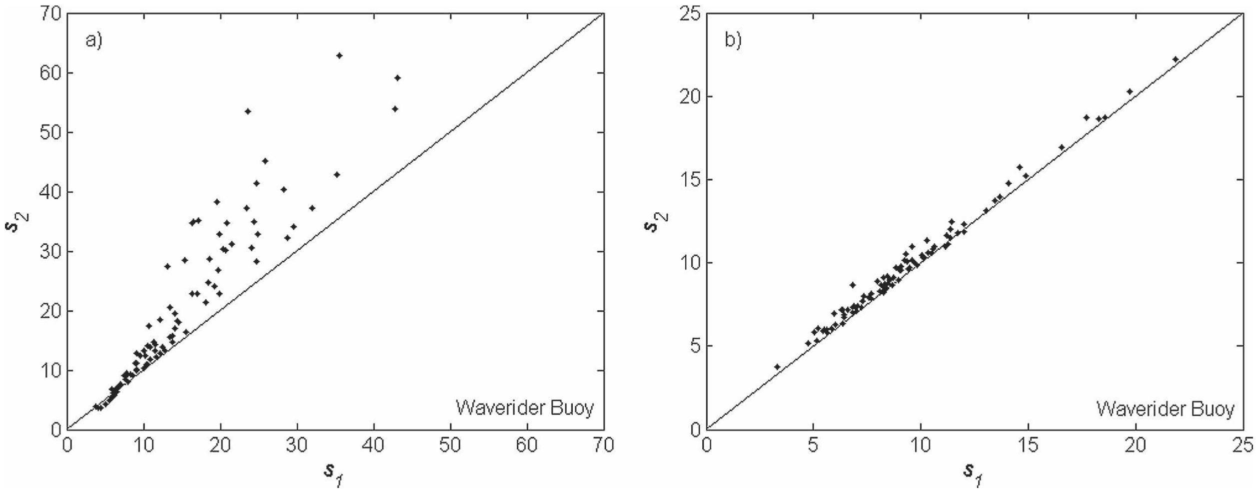

FIG. 8. The s_1 vs s_2 estimated from Waverider data using the (a) conventional approach and (b) proposed approach.

lated numerical tests, the consistency between s_1 and s_2 estimated using the proposed approach is excellent, with virtually all points falling near the diagonal line as shown in Fig. 8b. On the other hand, Fig. 8a shows that the consistency of the conventional approach is poor and s_2 is in general greater than s_1. Almost all of the estimated s falls in the range from 5 to 20 in using the proposed approach. While most estimated s using the conventional approach falls in that range, in about 18% of the cases, s_1 estimated using the conventional approach is significantly greater than 20, which is too great and hence may be erroneous. The consistency between θ_{M1} and θ_{M2} is satisfactory as observed in both Figs. 9a and 9b, although that given by the proposed approach is slightly better. The satisfactory consistency may partially result from the exclusion of the datasets in which the difference between θ_{M1} and θ_{M2}, estimated using the conventional approach, is greater than 10°. Although the trends observed in these two figures are based on the field measurements, they are very similar to those observed in the numerical tests.

b. *Estimation based on the PUV*

In applying the conventional approach, Eq. (3) was used to compute the Fourier coefficients, except that Q_{12} and Q_{13} are replaced by C_{12} and C_{13}, respectively, where subscripts 1, 2, and 3 denote wave pressure, and the x- and y-axis velocity components. The related results are plotted in Figs. 10 and 11. As observed in Figs. 10a and 10b, the consistency between s_1 and s_2 estimated using the proposed approach remains excellent, while that given by the conventional approach is rather poor. The estimated values of s_2 are in general greater, and some are significantly greater than those of s_1 in

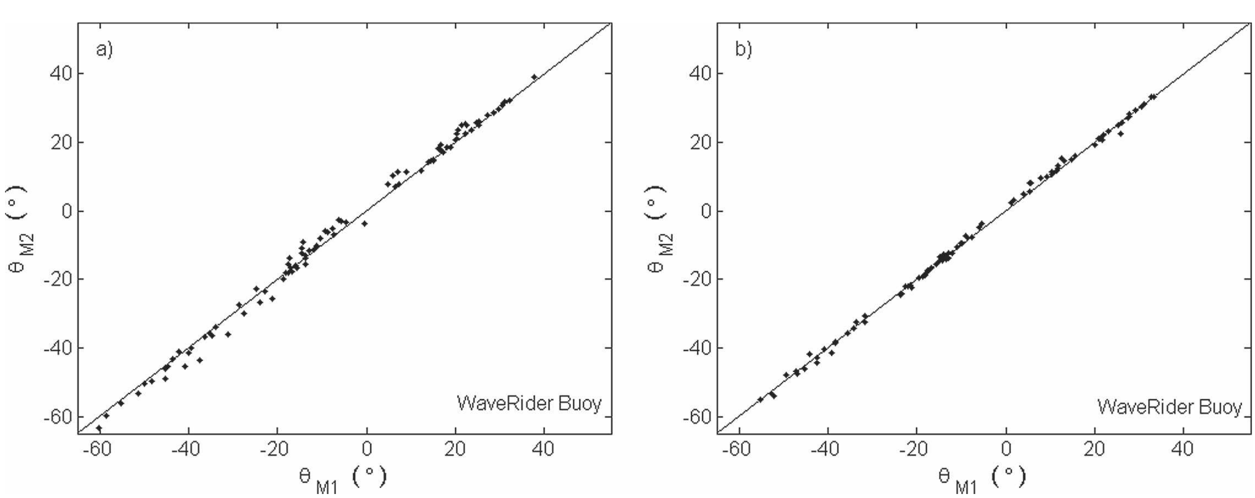

FIG. 9. The θ_{M1} vs θ_{M2} estimated from Waverider data using the (a) conventional approach and (b) proposed approach.

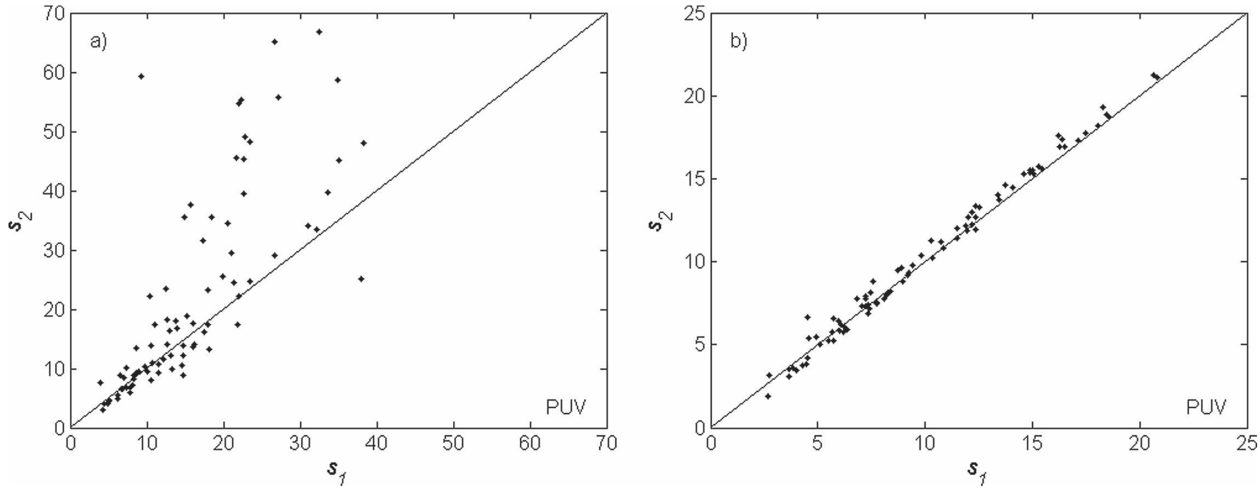

FIG. 10. The s_1 vs s_2 estimated from PUV data using the (a) conventional approach and (b) proposed approach.

using the conventional approach. The consistency between estimated θ_{M1} and θ_{M2} is satisfactory. In short, the general trends observed in the cases of the PUV records are similar to those in the cases of the Waverider records. However, the consistency of either approach is slightly deteriorated in comparison with the corresponding one in the case of the Waverider records.

c. *Spreading parameters at frequencies away from the spectral peaks*

To show that the proposed approach can also improve the estimate of the spreading parameters at frequencies other than the peak frequency, both approaches were applied to the estimate of the spreading parameters in the entire frequency domain for four Waverider records. The four cases are named as 9803051100, 9803051120, 9803050500, and 9803050520. The names refer to the starting time for the related measurements (yy/mm/dd/hh/mm). The significant wave heights, peak frequencies, and ratios of wind speed to phase velocity at the peak frequency (U_{10}/c_p) of these cases are summarized in Table 8.

The dependence of the spreading parameter on the frequency in all four cases is similar. For brevity, only the results of estimated s_1 and s_2 for case 9803051100 are presented in Figs. 12a and 12b, respectively, depicting the estimated s_1 and s_2 using the conventional and proposed approaches as a function of the frequency normalized by the peak frequency. For the purpose of comparison, also plotted in the figures is the empirical curve given by Hasselmann et al. (1980). It is observed that s_1 and s_2 estimated by both approaches reach the maximum near the peak frequency and decrease when

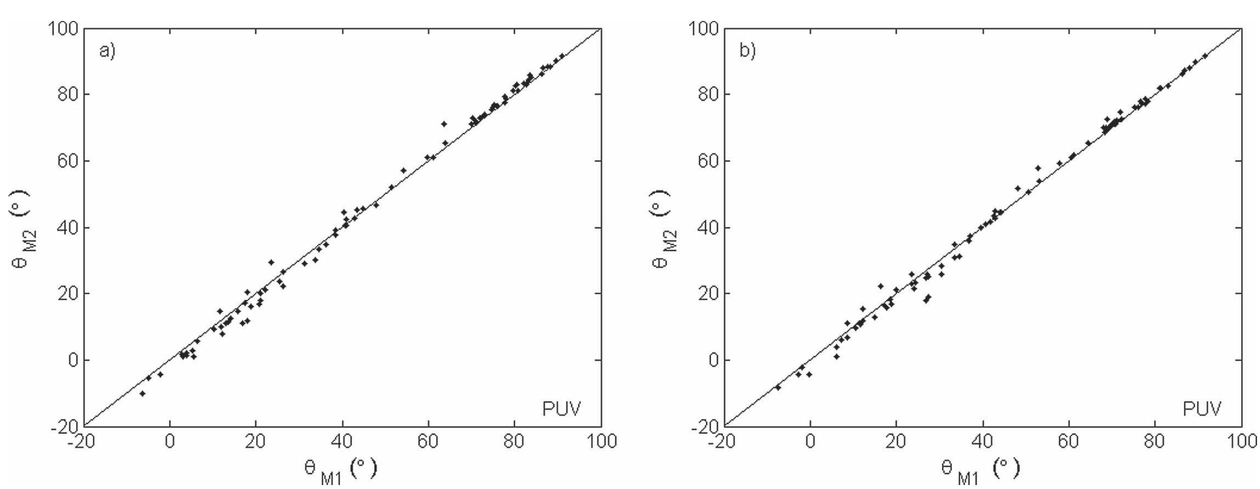

FIG. 11. The θ_{M1} vs θ_{M2} estimated from PUV data using the (a) conventional approach and (b) proposed approach.

TABLE 8. Sea states of selected four cases.

Case	$H_{1/3}$ (m)	f_p (Hz)	U_{10}/c_p
9803050500	3.39	0.1240	1.39
9803050520	3.42	0.1289	1.51
9803051100	3.42	0.1143	1.35
9803051120	3.10	0.1143	1.34

the frequency moves away from the spectral peak. They are in satisfactory agreement with the trend of the empirical curves fitted based on the Joint North Sea Wave Program (JONSWAP) data. It is also observed that both s_1 and s_2 fluctuate with respect to the empirical curves. Nevertheless, the fluctuation amplitude is much smaller in using the proposed approach.

To examine the consistency between estimated s_1 and s_2, we also compare the results of four cases in Fig. 13a for the conventional approach and Fig. 13b for the proposed approach. The figures clearly show that the consistency of s_1 and s_2 estimated using the proposed approach is superior, similar to that observed in sections 5a and 5b. In general, the estimated s_2 is much greater than s_1 in using the conventional approach. The consistency between s_1 and s_2 estimated using the proposed approach is excellent in the entire range of the spreading parameters, except for those of extremely small values ($s < 2$). The relatively large discrepancies mainly occur at very low or high frequency ranges where nonlinear second-order (difference frequency and sum frequency) bound waves are significant. It will be our future effort to find out whether or not the consistency can be improved after second-order bound waves are filtered from the measurements.

6. Conclusions

The accuracy and consistency of the proposed and conventional approaches were examined in estimating the mean wave direction and spreading parameter at the spectral peak of a wave field whose wave records were either numerically generated or measured in situ. In the case of the input being numerically generated wave records, the comparison between the estimates and the related prescribed values indicates that the proposed approach is statistically superior to the conventional approach, especially in estimating the directional spreading parameter. Namely, the former renders an almost unbiased mean and significantly smaller standard deviation in estimating the spreading parameter. When the field measurements were used as the input, the comparison between estimated s_1 and s_2 shows that the proposed approach results in substantially better consistency between them, which is consistent with the corresponding observation made in the numerical tests. Furthermore, the spreading parameters of waves at frequencies other than the peak frequency were also estimated using both approaches and are qualitatively consistent with the trend given by Hasselmann et al. (1980). The consistency between s_1 and s_2 estimated using the proposed approach at the frequencies other than the peak frequency is also found to be superior to that using the conventional approach. The consistency between estimated s_1 and s_2 is especially crucial in analyzing field measurements where the spreading parameter of a measured wave field is not known.

The employment of a data adaptive method (MLM) to estimate the directional spreading function and then its first two Fourier coefficients is the reason for the

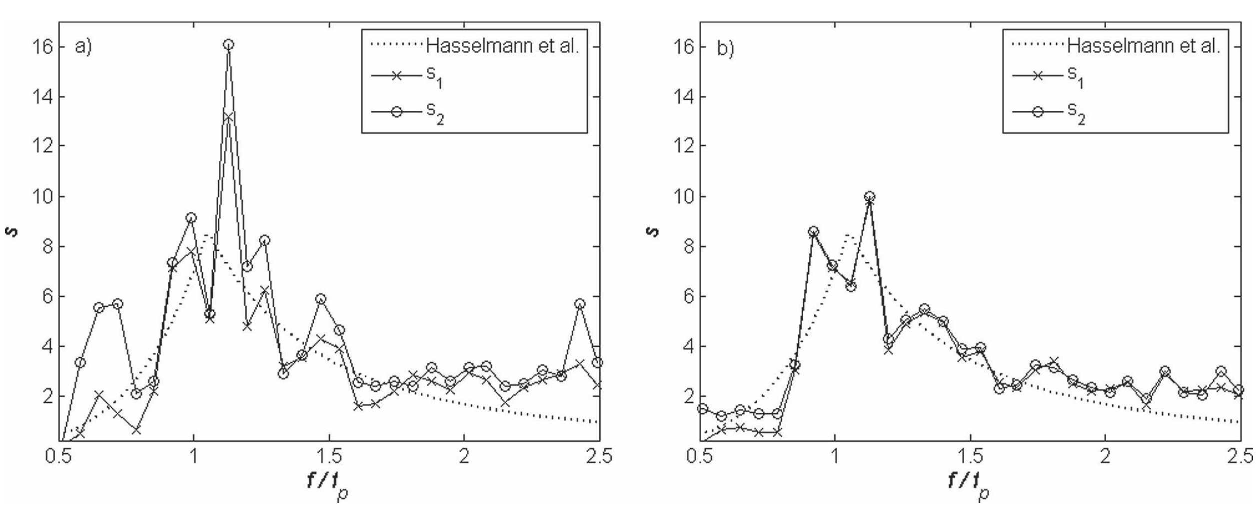

FIG. 12. Dependence of s on f/f_p for case 9803051100 (U_{10}/c_p = 1.35) using the (a) conventional approach and (b) proposed approach.

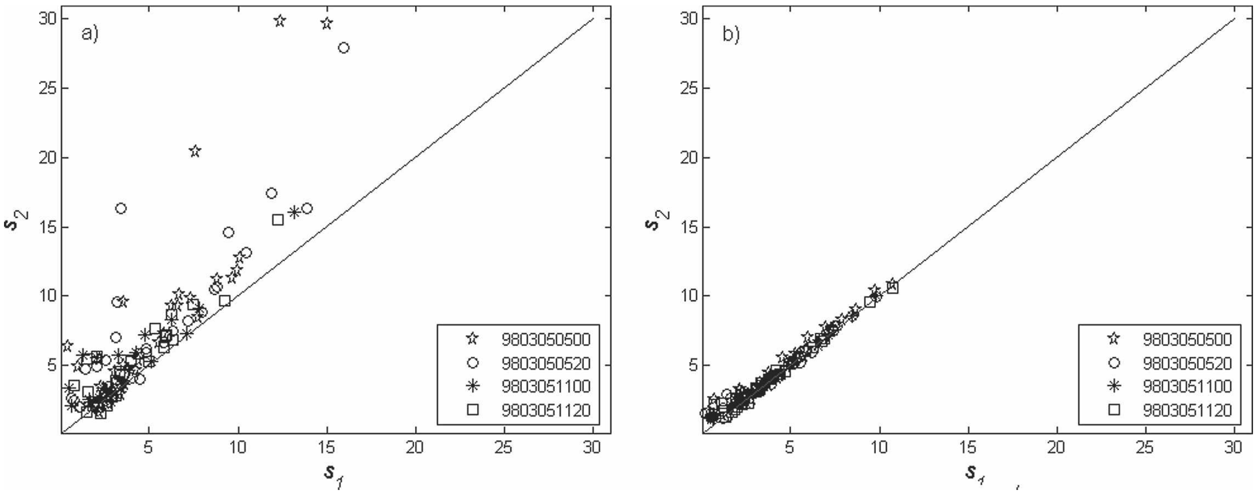

FIG. 13. Scatterplots of s_1 and s_2 estimated in the entire frequency domain using the (a) conventional approach and (b) proposed approach.

superiority of the proposed approach over the conventional approach. This is because an MLM is more tolerant of errors involved in the estimated cross-spectra than is the DFT used in the conventional approach. Although the average of the cross-spectra may reduce errors, especially those resulting from the "interaction" term, the reduction is limited by the duration of measured wave records and the requirements of resolution in the frequency domain. Hence, the use of the proposed approach in estimating the directional spreading coefficients of ocean wave is strongly recommended. Because a cosine-2s model is intended to model the sea states of unimode directional spreading and the efficacy of the proposed approach is only examined in these sea states in our study, it is not recommended to apply it to the sea states of a bi- and multimode.

Acknowledgments. The authors gratefully acknowledge the partial financial support provided by the Offshore Technology Research Center at Texas A&M University.

REFERENCES

Earle, M. D., 1996: Nondirectional and directional wave data analysis procedures. DNBC Tech. Doc. 96-01, 37 pp.

Ewing, J. A., and A. K. Laing, 1987: Directional spectra of seas near full development. *J. Phys. Oceanogr.,* **17,** 1696–1706.

Forristall, Z. G., and K. C. Ewans, 1998: Worldwide measurements of directional wave spreading. *J. Atmos. Oceanic Technol.,* **15,** 440–469.

——, and Coauthors, 2004: Wave crest sensor intercomparison study: An overview of WACSIS. *J. Offshore Mech. Arct. Eng.,* **126,** 26–34.

Harris, F. J., 1978: On the use of windows for harmonic analysis with the discrete Fourier transform. *Proc. IEEE,* **66,** 51–83.

Hashimoto, N., 1997: Analysis of the directional wave spectra from field data. *Advances in Coastal and Ocean Engineering,* Vol. 3, P.L.-F. Liu, Ed., World Scientific, 103–143.

Hasselmann, D. E., M. Dunckel, and J. A. Ewing, 1980: Directional wave spectra observed during JONSWAP 1973. *J. Phys. Oceanogr.,* **10,** 1264–1280.

Hwang, P. A., and D. W. Wang, 2000: Airborne measurements of the wavenumber spectra of ocean surface waves. Part II: Directional distribution. *J. Phys. Oceanogr.,* **30,** 2768–2787.

Isobe, M., K. Kondo, and K. Horikawa, 1984: Extension of MLM for estimating directional wave spectrum. *Proc. Symp. on Description and Modeling of Directional Seas*, Lyngby, Denmark, Danish Hydraulic Institute, A-6-1–A-6-15.

Jefferys, E. R., 1987: Directional sea should be ergodic. *Appl. Ocean Res.,* **9,** 186–191.

Jenkins, G. M., and D. G. Watts, 1968: *Spectra Analysis and Its Applications*. Holden Day, 525 pp.

Long, R. B., 1980: The statistical evaluation of directional spectrum estimates derived from pitch/roll buoy data. *J. Phys. Oceanogr.,* **10,** 944–952.

Longuet-Higgins, M. S., D. E. Cartwright, and N. D. Smith, 1963: Observations of the directional spectrum of sea waves using the motions of a floating buoy. *Ocean Wave Spectra*, Prentice Hall, 111–132.

Massel, S. R., and R. M. Brinkman, 1998: On the determination of directional wave spectra for practical applications. *Appl. Ocean Res.,* **20,** 357–374.

Miles, M. D., 1989: A note on directional random wave synthesis by the single summation method. *Proc. 23d IAHR Congress*, Vol. C, Ottawa, ON, Canada, IAHR, 243–250.

Mitsuyasu, H., F. Tasai, T. Suhara, S. Mizuno, M. Ohkusu, T. Honda, and K. Rikiishi, 1975: Observation of the directional spectrum of ocean waves using a cloverleaf buoy. *J. Phys. Oceanogr.,* **5,** 750–760.

Sand, S. E., and A. E. Mynett, 1987: Directional wave generation and analysis. *Proc. IAHR Seminar on Wave Analysis and*

Generation in Laboratory Basins, Lausanne, Switzerland, IAHR, 209–235.

Tucker, M. J., and E. G. Pitt, 2001: *Waves in Ocean Engineering*. Elsevier Science, 550 pp.

Wang, H. T., and C. B. Freise, 1997: Error analysis of the directional wave spectra obtained by the NDBC 3-m pitch-roll discus buoy. *IEEE J. Oceanic Eng.,* **22,** 639–648.

Welch, P. D., 1967: The use of fast Fourier transform for the estimation of power spectra: A method based on time averaging over short, modified periodgrams. *IEEE Trans. Audio Electroacoust.,* **AU-15,** 70–73.

Zhang, J., L. Chen, M. Ye, and R. E. Randall, 1996: Hybrid wave model for unidirectional irregular waves. Part I. Theory and numerical scheme. *Appl. Ocean Res.,* **18,** 77–92.

Zhang, S., and J. Zhang, 2004: Analysis of directional wave fields with strong current. *Appl. Ocean Res.,* **26,** 13–22.